Hindawi Publishing Corporation
EURASIP Journal on Applied Signal Processing
Volume 2006, Article ID 48789, Pages 1–13
DOI 10.1155/ASP/2006/48789

Mainlobe Jammer Nulling via TSI Finders: A Space Fast-time Adaptive Processor

Dan Madurasinghe and Andrew P. Shaw

Electronic Warfare and Radar Divison, Defence Science and Technology Organisation, P.O. Box 1500, Edinburgh, SA 5111, Australia

Received 17 October 2004; Revised 21 March 2005; Accepted 31 May 2005

An algorithm based on a space fast-time adaptive processor is presented for nulling the mainlobe jammer when the jammer and the target of interest share the same bearing. The computational load involved in the conventional processor, which blindly looks for the terrain-scattered interference (TSI), is required to stack a large number of consecutive range cell returns to form the space fast-time data snapshot making it almost impossible to implement in real time. This issue is resolved via the introduction of a preprocessor (a TSI finder which detects the presence of the minute levels of multipath components of the mainlobe jammer and associated time delays) which directs the STAP processor to select only two desired range returns in order to form the space fast-time data snapshot. The end result is a computationally extremely fast processor. Also a new space fast-time adaptive processor based on the super-resolution approach (eigenvector-based) is presented.

1. INTRODUCTION

Mainbeam jamming poses a difficult and challenging problem for the modern multichannel radar. Conventional processing techniques such as adaptive sidelobe cancelling or space-time adaptive processing (as in space slow-time adaptive processing) can successfully suppress the sidelobe jammers, where the space slow-time adaptive processing refers to the stacking of spatial data corresponding to a series of coherent pulses to form the space-time data snapshot for the range cell being interrogated [1]. This form of processing is very effective in achieving high spatio-temporal degrees of freedom to null sidelobe jammers and hot clutter. However when one of the jammers is colocated with the target of interest, these processors fail. A new emerging class of space-time processing techniques that may be referred to as space fast-time adaptive processing can overcome this problem. In space fast-time processing one needs only a minimum of one pulse in order to form a space fast-time processor by stacking a large number of range returns (fast-time samples) in the neighbourhood of the cell being interrogated. Success of the processor depends on the availability of coherent multipath in the form of terrain-scattered interference (TSI).

At present the known approaches [2–6] to solving this problem require one to stack a considerable number of range returns blindly to form the space fast-time data snapshot or apply a large number of filters first [6]. There are two main problems associated with the current approach. One is the size of the space fast-time covariance matrix which is very large, and its inversion which is computationally intensive. The second problem is the lack of training data to estimate it. In fact, in theory, one needs to consider one additional data snapshot corresponding to the time delay of one of the TSI paths (if the corresponding path delay is known).

In this study, first we develop a vector subspace-based approach to explain the procedure involved in nulling the mainlobe jammer, and secondly an eigenvector-based solution is presented alongside the currently used covariance matrix inversion-based solution. Finally a preprocessor is presented for identifying the availability of the TSI power and the associated path delays corresponding to the mainlobe jammer. This enables us to form the space fast-time data snapshot as a $2N \times 1$ vector by stacking the correct auxiliary range return (which corresponds to the TSI delay) with the current range cell of interest, where N is the number of array elements. As a result, the space fast-time covariance matrix need be formed only when TSI is present and its size is limited to $2N \times 2N$. The TSI finder, unlike the conventional direction finder, does not estimate the angle of arrival of the TSI paths, instead it estimates the path delays associated with each coherent multipath off the mainlobe jammer while suppressing the mainlobe jammer itself and all of the sidelobe

jammers which are uncorrelated with the mainlobe jammer. Furthermore, we have derived the expression for the achievable signal processing gain as a function of the power level of the TSI path being used to null the mainlobe jammer. This would provide us with some insight into understanding the ability of the processor, particularly its limitations. Since the bulk of the computational load has been lifted, this innovative preprocessor will allow a modern radar to implement an ultimate adaptive processor, that is, the space slow-time fast-time adaptive processor, to null sidelobe jammers, mainlobe jammer, and hot clutter in a single processor within a realistic time frame. The order of the computational load is reduced from $(NMR)^3$ to $(2NM)^3$ where M is the number of coherent pulses and R is the number of fast-time range cells to be used (R is generally unknown, but large) in order to form the space fast-time component of the data vector.

2. FORMULATION

Suppose an N-channel radar, whose $N \times 1$ steering manifold is represented by $s(\phi, \theta)$ (where ϕ is the azimuth angle and θ is the elevation angle), transmits a single pulse where $\mathbf{s}(\phi,\theta)^H \mathbf{s}(\phi,\theta) = N$ and the superscript H denotes the Hermitian transpose. The return (i.e., the $N \times 1$ measured signal $\mathbf{x}(r)$) corresponding to the rth range gate (which is also referred to as the fast-time scale) can be written as

$$\mathbf{x}(r) = \alpha_t \delta(r - r_0)\mathbf{s}(\phi_t, \theta_t) + j(r)\mathbf{s}(\phi_t, \theta_t) + \sum_{k=1}^{k=K} \beta_k j(r - n_k)\mathbf{s}(\phi_k, \theta_k) + \boldsymbol{\varepsilon}, \tag{1}$$

where α_t is the target amplitude, r_0 is the target range cell number, δ represents the Kronecker delta function, $j(r)$ represents a series of complex random amplitudes corresponding to the mainlobe jammer, (ϕ_t, θ_t) is the bearing of the target as well as the mainlobe jammer. The third term (summation term) consists of K multipath arrivals known as terrain-scattered interferers (TSI), where the integers n_k $(k = 1, 2, \ldots, K)$ are the associated path delays (lags), $\mathbf{s}(\phi_k, \theta_k)$ $(k = 1, 2, \ldots, K)$ are the corresponding steering vectors, β_k $(k = 1, 2, \ldots, K)$ are the scattering coefficients $(|\beta_k|^2 < 1)$, and $\boldsymbol{\varepsilon}$ represents the $N \times 1$ white noise component. In this study we consider the clutter-free case. Furthermore, we assume $\sigma_j^2 = E\{|j(r)|^2\}$ is the power level of the mainlobe jammer and $|\beta_k|^2\sigma_j^2$ $(k = 1, 2, \ldots, K)$ represent the TSI power levels associated with each multipath, where $E\{\cdot\}$ denotes the expectation operator with respect to the variable r. Throughout the analysis, we assume that the mainlobe jammer power is above the channel noise power, that is, Jnr $= \sigma_j^2/\sigma_n^2 > 1$, $E\{\boldsymbol{\varepsilon}\boldsymbol{\varepsilon}^H\} = \sigma_n^2 \mathbf{I}_N$ where Jnr is the jammer-to-noise ratio per channel, σ_n^2 is the white noise power present in any channel, and $\mathbf{I}_N$ is the unit identity matrix. Without loss of generality, we use the notation $\mathbf{s}_t$ and $\mathbf{s}_k$ to represent $\mathbf{s}(\phi_t, \theta_t)$ and $\mathbf{s}(\phi_k, \theta_k)$, respectively. Furthermore, it is assumed that $E\{j(r + l)j(r + m)^*\} = \sigma_j^2 \delta(l - m)$, where * denotes the complex conjugate operation. It should also be noted that it is possible to have additional independent jammers added to the expression in (1). This will be equivalent to an additional term $\sum_{k=1}^{Q} \hat{j}_k(r)\hat{\mathbf{s}}_k$ due to Q sidelobe jammers, where $\hat{j}_k(r)$ are the associated random amplitudes and $\hat{\mathbf{s}}_k = \mathbf{s}(\hat{\phi}_k, \hat{\theta}_k)$, $(k = 1, 2, \ldots, Q)$ are the corresponding steering vectors. The presence of these sidelobe jammers does not alter the theory to follow.

2.1. Vector subspace-based approach

The $N \times N$ interference covariance matrix formed by summing and averaging the outer products $\mathbf{x}\mathbf{x}^H$ has the following properties. Its signal subspace, which is a subspace of complex N-dimensional space (or $\mathbf{C}^{N\times 1}$) formed by the base vectors $\mathbf{s}_t$ and $\mathbf{s}_k$ $(k = 1, 2, \ldots, K)$ is $K + 1$ dimensional and its noise subspace is of dimension $N - (K + 1)$. Generally the range cell which is being interrogated for targets (in this case $r = r_0$) would not be included in forming the covariance matrix. However, due to the fact that the mainlobe jammer is associated with the same steering vector as the target, we are forced to include $\mathbf{s_t}$ in the signal subspace. Alternatively suppose that we have only sidelobe jammers, then $\mathbf{s}_t$ is not a member of the signal subspace. In this case (i.e., mainlobe jammer-free case) the objective is to find an $N \times 1$ weights vector $\mathbf{w}$ which is orthogonal to the signal subspace and satisfies the condition $\mathbf{w}^H\mathbf{s}_t = 1$ (such a solution is always available via the eigenvector-based high-resolution approach as seen later). The orthogonality requirement guarantees that the weights vector is orthogonal to steering vectors associated with all interferers and as a result, when applied to the range cell of interest, we have $\mathbf{w}^H\mathbf{x}(r) = \alpha_t\delta(r - r_0) + \mathbf{w}^H\boldsymbol{\varepsilon}$ (note: $\mathbf{w}^H\hat{\mathbf{s}}_k = 0$ is guaranteed for sidelobe arrivals). This is simply a spatial beamformer. On the other hand, when a mainlobe jammer is present, suppose we are still able to find a weights vector which is orthogonal to all the basis vectors in the signal subspace, that is, $\mathbf{w}^H\mathbf{s}_k = 0$, $\mathbf{w}^H\hat{\mathbf{s}}_k = 0$, excluding the vector $\mathbf{s}_t$ for which we maintain the look direction constraint $\mathbf{w}^H\mathbf{s}_t = 1$ (such a solution is also available via the power minimization approach which can make the weights vector almost orthogonal to the undesired steering vectors in the signal subspace). Then the beamformer output is given by $\mathbf{w}^H\mathbf{x}(r) = \alpha_t\delta(r - t_0) + j(r) + \mathbf{w}^H\boldsymbol{\varepsilon}$ which incorporate the mainlobe jammer data. This is the fundamental reason for the failure of the spatial beamformer whenever a mainlobe jammer is present.

In order to understand the space fast-time adaptive processor, let us consider a $4N \times 1$ space fast-time data snapshot by stacking 4 consecutive range cell returns. The $4N \times 1$ data vector has the form

$$\mathbf{y}(r) = \left(\mathbf{x}(r)^T, \mathbf{x}(r + 1)^T, \mathbf{x}(r + 2)^T, \mathbf{x}(r + 3)^T\right)^T. \tag{2}$$

The $4N \times 4N$ covariance matrix is defined as the average sum of the outer products of $\mathbf{y}(r)\mathbf{y}(r)^H$. Suppose $\mathbf{x}(r) = \alpha_t\delta(r - r_0)\mathbf{s}_t + j(r)\mathbf{s}_t + \beta_k j(r - n_k)\mathbf{s}_k + \boldsymbol{\varepsilon}$ (target, mainlobe jammer, and any one of the TSI paths), then the data snapshot has the

following structure:

$$\begin{aligned}
&\mathbf{y}(r)\\
&\quad=\alpha_t\delta(r-r_0)\left(\mathbf{s}_t^T,\mathbf{o}^T,\mathbf{o}^T,\mathbf{o}^T\right)^T\\
&\qquad+j(r)\left(\mathbf{s}_t^T,\mathbf{o}^T,\mathbf{o}^T,\mathbf{o}^T\right)^T\\
&\qquad+(r+1)\left(\mathbf{o}^T,\mathbf{s}_t^T,\mathbf{o}^T,\mathbf{o}^T\right)^T\\
&\qquad+j(r+2)\left(\mathbf{o}^T,\mathbf{o}^T,\mathbf{s}_t^T,\mathbf{o}^T\right)^T\\
&\qquad+j(r+3)\left(\mathbf{o}^T,\mathbf{o}^T,\mathbf{o}^T,\mathbf{s}_t^T\right)^T\\
&\qquad+\beta_k j(r-n_k)\left(\mathbf{s}_k^T,\mathbf{o}^T,\mathbf{o}^T,\mathbf{o}^T\right)^T\\
&\qquad+\beta_k j(r+1-n_k)\left(\mathbf{o}^T,\mathbf{s}_k^T,\mathbf{o}^T,\mathbf{o}^T\right)^T\\
&\qquad+\beta_k j(r+2-n_k)\left(\mathbf{o}^T,\mathbf{o}^T,\mathbf{s}_k^T,\mathbf{o}^T\right)^T\\
&\qquad+\beta_k j(r+3-n_k)\left(\mathbf{o}^T,\mathbf{o}^T,\mathbf{o}^T,\mathbf{s}_k^T\right)^T\\
&\qquad+\mathbf{e},
\end{aligned}\tag{3}$$

where $\mathbf{o}=(0,0,\ldots,0,0)^T$ is the $N\times 1$ vector of zeros and $\mathbf{e}$ represent the $4N\times 1$ noise component. The signal subspace which is a subspace of $\mathbf{C}^{4N\times 1}$ is represented by the linearly independent basis vectors $(\mathbf{s}_t^T,\mathbf{o}^T,\mathbf{o}^T,\mathbf{o}^T)^T$, $(\mathbf{o}^T,\mathbf{s}_t^T,\mathbf{o}^T,\mathbf{o}^T)^T$, $(\mathbf{o}^T,\mathbf{o}^T,\mathbf{s}_t^T,\mathbf{o}^T)^T$, $(\mathbf{o}^T,\mathbf{o}^T,\mathbf{o}^T,\mathbf{s}_t^T)^T$, $(\mathbf{s}_k^T,\mathbf{o}^T,\mathbf{o}^T,\mathbf{o}^T)^T$, $(\mathbf{o}^T,\mathbf{s}_k^T,\mathbf{o}^T,\mathbf{o}^T)^T$, $(\mathbf{o}^T,\mathbf{o}^T,\mathbf{s}_k^T,\mathbf{o}^T)^T$, and $(\mathbf{o}^T,\mathbf{o}^T,\mathbf{o}^T,\mathbf{s}_k^T)^T$. As before the vector corresponding to the target, that is, $(\mathbf{s}_t^T,\mathbf{o}^T,\mathbf{o}^T,\mathbf{o}^T)^T$ is contained in the signal subspace of the covariance matrix. However, suppose n_k is equal to one of the integers between 1 and 4, then we would have a signal subspace which will not contain $(\mathbf{s}_t^T,\mathbf{o}^T,\mathbf{o}^T,\mathbf{o}^T)^T$ as a basis vector. For example, suppose $n_k=2$ (i.e., $j(r)\equiv j(r+2-n_k)$), then the signal subspace is formed by the basis vectors $(\mathbf{s}_t^T,\mathbf{o}^T,\beta_k\mathbf{s}_k^T,\mathbf{o}^T)^T$, $(\mathbf{o}^T,\mathbf{s}_t^T,\mathbf{o}^T,\mathbf{o}^T)^T$, $(\mathbf{o}^T,\mathbf{o}^T,\mathbf{s}_t^T,\mathbf{o}^T)^T$, $(\mathbf{o}^T,\mathbf{o}^T,\mathbf{o}^T,\mathbf{s}_t^T)^T$, $(\mathbf{s}_k^T,\mathbf{o}^T,\mathbf{o}^T,\mathbf{o}^T)^T$, $(\mathbf{o}^T,\mathbf{s}_k^T,\mathbf{o}^T,\mathbf{o}^T)^T$, and $(\mathbf{o}^T,\mathbf{o}^T,\mathbf{o}^T,\mathbf{s}_k^T)^T$. This omission of $(\mathbf{s}_t^T,\mathbf{o}^T,\mathbf{o}^T,\mathbf{o}^T)^T$ as a contributing vector to form the signal subspace occurs whenever $\beta_k\neq 0$ for some k $(1\leqslant n_k\leqslant 3)$. In this case if we compute the $4N\times 1$ weights vector orthogonal to the signal subspace, satisfying the requirement $\mathbf{w}^H(\mathbf{s}_t^T,\mathbf{o}^T,\mathbf{o}^T,\mathbf{o}^T)^T=1$, then we have the required space fast-time adaptive processor output $\mathbf{w}^H\mathbf{y}(r)=\alpha_T\delta(r-r_0)+\mathbf{w}^H\mathbf{e}$. It is clearly seen that we may need to stack a large number of range returns (several hundred) in order to blindly exploit the opportunity to null the mainlobe jammer energy at the processor output. This will not only increase the dimension of the covariance matrix to a very high value, it also makes it virtually impossible to form an accurate interference covariance matrix due to lack of training cells. It should also be noted that to null the mainlobe jammer (i.e., to exclude the target steering vector in signal subspace), all we need is to match the time delay of any one of the TSI paths available. On the other hand if none of the TSI paths is able to have a matching path delay in the selected stack, our signal steering vector $(\mathbf{s}_t^T,\mathbf{o}^T,\mathbf{o}^T,\mathbf{o}^T)^T$ is included in the signal subspace. In this case if we compute a weights vector orthogonal to the steering vectors in the signal subspace excluding the vector $(\mathbf{s}_t^T,\mathbf{o}^T,\mathbf{o}^T,\mathbf{o}^T)^T$, where we maintain the look direction constraint, then the processor output is $\mathbf{w}^H\mathbf{y}(r)=\alpha_T\delta(r-r_0)+j(r)+\mathbf{w}^H\mathbf{e}$.

2.2. The preprocessor approach

The first objective of this study is to simplify the above concept of blind inclusion of the large number of range cell returns to form an unnecessarily high-dimensional space fast-time adaptive processor. Suppose we have a preprocessor that determines the number of multipaths available (TSI off the mainlobe jammer only) and associated time delays. As an example assume that at least one such TSI is known to have a delay path of m units. Suppose the associated unknown steering vector for this path is $\mathbf{s}_m$, then the $2N\times 1$ space fast-time data snapshot is defined as $\mathbf{y}(r)=(\mathbf{x}(r)^T,\mathbf{x}(r+m)^T)^T$ where the dimensionality of the processor will always be $2N$. The form of the measured signal is (ignoring other multipaths and sidelobe jammers by assuming that they can be spatially nulled)

$$\begin{aligned}
\mathbf{y}(r)=\alpha_t\delta(r-r_0)\left(\mathbf{s}_t^T,\mathbf{o}^T\right)^T+j(r)\left(\mathbf{s}_t^T,\beta\mathbf{s}_m^T\right)^T\\
+j(r+m)\left(\mathbf{o}^T,\mathbf{s}_t^T\right)+\beta j(r-m)\left(\mathbf{s}_m^T,\mathbf{o}^T\right)^T+\mathbf{e}.
\end{aligned}\tag{4}$$

The signal subspace consists of the basis vectors $(\mathbf{s}_t^T,\beta\mathbf{s}_m^T)^T$, $(\mathbf{o}^T,\mathbf{s}_t^T)^T$, $(\mathbf{s}_m^T,\mathbf{o}^T)^T$, and other linearly independent vectors, that is, $(\mathbf{o}^T,\mathbf{s}_k^T)^T$, $(\mathbf{s}_k^T,\mathbf{o}^T)^T$, $k=1,2,\ldots,K$, $k\neq m$, arising from other TSI paths, and $(\mathbf{o}^T,\hat{\mathbf{s}}_k^T)^T$, $(\hat{\mathbf{s}}_k^T,\mathbf{o}^T)^T$, $k=1,2,\ldots,Q$ due to other sidelobe jammers. For the sake of brevity, we continue to ignore sidelobe jammers and multiple TSI paths. The exclusion of the desired signal related steering vector, that is, $(\mathbf{s}_t^T,\mathbf{o}^T)^T$, in the signal subspace, will enable us to extract the signal of interest as discussed earlier.

3. POSSIBLE SOLUTIONS

3.1. Subspace-based solution

The subspace solution (the high-resolution approach) depends on the eigen analysis of the $2N\times 2N$ covariance matrix, whose eigenvectors corresponding to the largest eigenvalues are known as signal subspace eigenvectors [7]. The rest of the eigenvectors are termed as noise eigenvectors. A property of the signal subspace eigenvectors is that they form a basis for the signal subspace which is also spanned by the vectors $(\mathbf{s}_t^T,\beta\mathbf{s}_m^T)^T$, $(\mathbf{o}^T,\mathbf{s}_t^T)^T$, $(\mathbf{s}_m^T,\mathbf{o}^T)^T$. Now suppose $\mathbf{E}_1$, $\mathbf{E}_2$, $\mathbf{E}_3$ are the signal subspace eigenvectors (more details of separating the signal subspace eigenvectors are given in [7]). The orthogonality requirement is equivalent to $\mathbf{w}^H\mathbf{E}_k=0$ $(k=1,2,3)$. If more eigenvectors are found in the signal subspace, this implies the presence of other TSI paths and sidelobe jammers. In order to achieve the lowest possible sidelobes in the final pattern while satisfying the orthogonality requirement, we will minimise $\mathbf{w}^H\mathbf{w}$ subject to the conditions $\mathbf{w}^H(\mathbf{s}_t^T,\mathbf{o}^T)^T=1.0$ and $\mathbf{w}^H\mathbf{E}_k=0$ $(k=1,2,\ldots,q)$, where q is the dimension of the signal subspace. This leads to

the minimisation of the following objective function:

$$\Phi(\mathbf{w}) = \mathbf{w}^H\mathbf{w} + \lambda(\mathbf{w}^H\mathbf{s}_A - 1) + \sum_{k=1}^{q} \mu_k \mathbf{w}^H\mathbf{E}_k, \tag{5}$$

where $\lambda, \mu_1, \mu_2, \ldots, \mu_K$ are scalar quantities (Lagrange multipliers) which correspond to the minimum value of Φ and $\mathbf{s}_A = (\mathbf{s}_t^T, \mathbf{o}^T)^T$ represents the space fast-time look direction steering vector. By differentiating Φ with respect to $\mathbf{w}^H$ and equating to zero, we have

$$\mathbf{w} + \lambda\mathbf{s}_A + \sum_{k=1}^{q} \mu_k \mathbf{E}_k = 0. \tag{6}$$

The weight vector is given by

$$\mathbf{w} = -\lambda\mathbf{s}_A - \sum_{k=1}^{q} \mu_k \mathbf{E}_k. \tag{7}$$

Now applying $\mathbf{w}^H\mathbf{E}_m = 0$ $(m = 1, 2, \ldots, q)$, we have

$$\lambda^*\mathbf{s}_A^H\mathbf{E}_m + \sum_{k=1}^{q} \mu_k^*\mathbf{E}_k^H\mathbf{E}_m = 0, \quad m = 1, 2, \ldots, q. \tag{8}$$

The look direction constraint $\mathbf{w}^H\mathbf{s}_A = 1$ implies

$$\lambda^*\mathbf{s}_A^H\mathbf{s}_A + \sum_{k=1}^{q} \mu_k^*\mathbf{E}_k^H\mathbf{s}_A = -1. \tag{9}$$

By combining (8) and (9), we can estimate the unknown parameters $\mathbf{U} = (\lambda^*, \mu_1^*, \ldots, \mu_q^*)^T$ using the following linear system:

$$\begin{pmatrix} \mathbf{s}_A^H\mathbf{s}_A & (\mathbf{B}^H\mathbf{s}_A)^T \\ (\mathbf{s}_A^H\mathbf{B})^T & (\mathbf{B}^H\mathbf{B})^T \end{pmatrix} \mathbf{U} = \begin{pmatrix} -1 \\ \mathbf{o}_{q\times 1} \end{pmatrix}, \tag{10}$$

where $\mathbf{B} = (\mathbf{E}_1, \mathbf{E}_2, \ldots, \mathbf{E}_q)$ and $\mathbf{o}_{q\times 1}$ is a $q \times 1$ column vector of zeros.

3.2. Minimum power distortionless response solution for space fast-time adaptive processing

The MPDR [1] solution minimises the power output of the objective function $\mathbf{w}^H\mathbf{R}\mathbf{w}$, where $\mathbf{R}$ is the $2N \times 2N$ measured space fast-time covariance matrix, subject to the constraint $\mathbf{w}^H(\mathbf{s}_t^T, \mathbf{o}^T)^T = 1$. The conventional MPDR solution needs to be slightly altered due to the fact that we can impose additional constraints using the following argument. Ideally, as discussed earlier, we would like to satisfy $\mathbf{w}^H(\mathbf{s}_t^T, \mathbf{o}^T)^T = 1$ as the constraint and maintain the orthogonality: $\mathbf{w}^H(\mathbf{o}^T, \mathbf{s}_t^T)^T = 0$, $\mathbf{w}^H(\mathbf{s}_m^T, \mathbf{o}^T)^T = 0$, $\mathbf{w}^H(\mathbf{s}_t^T, \beta\mathbf{s}_m^T)^T = 0$, $\mathbf{w}^H(\mathbf{s}_k^T, \mathbf{o}^T)^T = 0$, $\mathbf{w}^H(\mathbf{o}^T, \mathbf{s}_k^T)^T = 0$ $(k = 1, 2, \ldots, K,\ k \neq m)$, $\mathbf{w}^H(\hat{\mathbf{s}}_k^T, \mathbf{o}^T)^T = 0$, $\mathbf{w}^H(\mathbf{o}^T, \hat{\mathbf{s}}_k^T)^T = 0$ $(k = 1, 2, \ldots, Q)$, and so forth. Since we have the full knowledge of the vector $(\mathbf{o}^T, \mathbf{s}_t^T)^T$, the orthogonality requirement arising from this vector (this is not the signal steering vector in space fast-time domain) can be enforced as an additional constraint: $\mathbf{w}^H(\mathbf{o}^T, \mathbf{s}_t^T)^T = 0$ in the power minimization procedure to achieve a better result. Thus we would like to minimise the following objective function:

$$\Phi_M(\mathbf{w}) = \mathbf{w}^H\mathbf{R}\mathbf{w} + \lambda\left(\mathbf{w}^H(\mathbf{s}_t^T, \mathbf{o}^T)^T - 1\right) + \mu\mathbf{w}^H(\mathbf{o}^T, \mathbf{s}_t^T)^T. \tag{11}$$

This solution is always available (for a fixed m), regardless of whether the signal steering vector $(\mathbf{s}_t^T, \mathbf{o}^T)^T$ is included in the signal subspace of the covariance matrix or not, in other words, whether β_m has a zero value or not. The weights vector is given by $\mathbf{w} = -\lambda\mathbf{R}^{-1}\mathbf{s}_A - \mu\mathbf{R}^{-1}\mathbf{s}_B$, where $\mathbf{s}_A = (\mathbf{s}_t^T, \mathbf{o}^T)^T$, $\mathbf{s}_B = (\mathbf{o}^T, \mathbf{s}_t^T)^T$, and the parameters λ and μ are given by

$$\begin{pmatrix} \mathbf{s}_A^H\mathbf{R}^{-1}\mathbf{s}_A & \mathbf{s}_B^H\mathbf{R}^{-1}\mathbf{s}_A \\ \mathbf{s}_A^H\mathbf{R}^{-1}\mathbf{s}_B & \mathbf{s}_B^H\mathbf{R}^{-1}\mathbf{s}_B \end{pmatrix} \begin{pmatrix} \lambda^* \\ \mu^* \end{pmatrix} = \begin{pmatrix} -1 \\ 0 \end{pmatrix}. \tag{12}$$

In general, $\mathbf{w}$ is not orthogonal to all the steering vectors in the signal subspace. Naturally the weights vector is almost orthogonal to all the steering vectors included in the signal subspace except for the one specified in the look direction constraint. Therefore, if for some reason the selected TSI path is not sufficiently strong, or if the selected path delay is not available as a TSI, the end result is that the mainlobe jammer is associated with the desired signal steering vector $(\mathbf{s}_t^T, \mathbf{o}^T)^T$ (instead of $(\mathbf{s}_t^T, \beta\mathbf{s}_m^T)^T$). However, the weights vector will be almost orthogonal to all other steering vectors (except $(\mathbf{s}_t^T, \mathbf{o}^T)^T$). In this case, the output at the processor will be dominated by a series of random numbers corresponding to the mainlobe jammer, that is, $\mathbf{w}^H\mathbf{x}(r) = \alpha_t\delta(r - r_0) + j(r) + \mathbf{w}^H\boldsymbol{\varepsilon}$. Further analysis of this solution is carried in the next section by investigating the nature of the $2N \times 1$ weights vector.

4. PROPERTIES OF THE MPDR SOLUTION

Under the fundamental assumption that we have identified the path delay corresponding to at least one TSI (i.e., m), we can compute the $2N \times 2N$ covariance matrix using (4) as

$$\mathbf{R} = \begin{pmatrix} \mathbf{R}_x & \sigma_f^2\beta_m^*\mathbf{s}_t\mathbf{s}_m^H \\ \sigma_f^2\beta_m\mathbf{s}_m\mathbf{s}_t^H & \mathbf{R}_x \end{pmatrix}, \tag{13}$$

where $\mathbf{R}_x = \sigma_f^2\mathbf{s}_t\mathbf{s}_t^H + \mathbf{R}_1$ is the $N \times N$ measured spatial covariance matrix estimated as the average of outer product terms $\mathbf{x}(r)\mathbf{x}(r)^H$ and $\mathbf{R}_1 = \sigma_f^2|\beta_m|^2\mathbf{s}_m\mathbf{s}_m^H + \sigma_n^2\mathbf{I}_N$ is not a measurable quantity using data.

Note that when other TSI paths and sidelobe jammers are taken into account, the only difference is that

$$\mathbf{R}_1 = \sigma_f^2\,|\beta_m|^2\,\mathbf{s}_m\mathbf{s}_m^H + \sigma_n^2\mathbf{I}_N + \left(\sum_{k=1}^{m-1} \sigma_f^2\,|\beta_k^2|\,\mathbf{s}_k\mathbf{s}_k^H + \sum_{k=m+1}^{K} \sigma_f^2\,|\beta_k^2|\,\mathbf{s}_k\mathbf{s}_k^H + \sum_{k=1}^{Q} \hat{\sigma}_f^2\hat{\mathbf{s}}_k\hat{\mathbf{s}}_k^H\right). \tag{14}$$

Now, for the sake of convenience, we represent the $2N\times 1$ weights vector as $\mathbf{w}^T = (\mathbf{w}_1^T, \mathbf{w}_2^T)^T$, where $N \times 1$ vector $\mathbf{w}_1$ refers to the first N components of $\mathbf{w}$ and the rest is represented by $N\times 1$ vector $\mathbf{w}_2$. The output power at the processor P_{out} is given by

$$\begin{aligned} P_{\text{out}} &= \mathbf{w}^H\mathbf{R}\mathbf{w} \\ &= \mathbf{w}_1^H\mathbf{R}_1\mathbf{w}_1 + \mathbf{w}_2^H\mathbf{R}_1\mathbf{w}_2 + \sigma_J^2\mathbf{w}_1^H\mathbf{s}_t\mathbf{s}_t^H\mathbf{w}_1 + \sigma_J^2\mathbf{w}_2^H\mathbf{s}_t\mathbf{s}_t^H\mathbf{w}_2 \\ &\quad + \sigma_J^2\beta_m^*\mathbf{w}_1^H\mathbf{s}_t\mathbf{s}_m^H\mathbf{w}_2 + \sigma_J^2\beta_m\mathbf{w}_2^H\mathbf{s}_m\mathbf{s}_t^H\mathbf{w}_1. \end{aligned} \tag{15}$$

The constraints $\mathbf{w}^H(\mathbf{s}_t^T, \mathbf{o}^T)^T = 1$ and $\mathbf{w}^H(\mathbf{o}^T, \mathbf{s}_t^T)^T = 0$ are, in fact, equivalent to $\mathbf{w}_1^H\mathbf{s}_t = 1$ and $\mathbf{w}_2^H\mathbf{s}_t = 0$. As a result, we may substitute these requirements into $\mathbf{w}^H\mathbf{R}\mathbf{w}$ to obtain

$$\begin{aligned} P_{\text{out}} &= \mathbf{w}^H\mathbf{R}\mathbf{w} \\ &= \mathbf{w}_1^H\mathbf{R}_1\mathbf{w}_1 + \mathbf{w}_2^H\mathbf{R}_1\mathbf{w}_2 + \sigma_J^2 + \sigma_J^2(\beta_m^*\mathbf{s}_m^H\mathbf{w}_2 + \beta_m\mathbf{w}_2^H\mathbf{s}_m). \end{aligned} \tag{16}$$

The original power minimization problem can now be broken into two independent optimisation problems as follows:

(1) minimise $\mathbf{w}_1^H\mathbf{R}_1\mathbf{w}_1$ subject to the constraint $\mathbf{w}_1^H\mathbf{s}_t = 1$,
(2) minimise $\mathbf{w}_2^H\mathbf{R}_1\mathbf{w}_2 + \sigma_J^2 + \sigma_J^2(\beta_m^*\mathbf{s}_m^H\mathbf{w}_2 + \beta_m\mathbf{w}_2^H\mathbf{s}_m)$ subject to $\mathbf{w}_2^H\mathbf{s}_t = 0$.

The MPDR solution can be expressed as

$$\mathbf{w}_1 = \frac{\mathbf{R}_1^{-1}\mathbf{s}_t}{(\mathbf{s}_t^H\mathbf{R}_1^{-1}\mathbf{s}_t)}, \tag{17}$$

$$\mathbf{w}_2 = -\beta_m\sigma_J^2\mathbf{R}_1^{-1}\mathbf{s}_m + \beta_m\sigma_J^2\left(\frac{\mathbf{s}_t^H\mathbf{R}_1^{-1}\mathbf{s}_m}{\mathbf{s}_t^H\mathbf{R}_1^{-1}\mathbf{s}_t}\right)\mathbf{R}_1^{-1}\mathbf{s}_t. \tag{18}$$

The above representation of the MPDR solution cannot be used to compute the weights vector $\mathbf{w}$ due to the fact that the quantities involved are not measurable. Direct approach (11) is implemented to evaluate $\mathbf{w}$ as described in the previous section. Substituting $\mathbf{R}_1 = \sigma_J^2|\beta_m|^2\mathbf{s}_m\mathbf{s}_m^H + \sigma_n^2\mathbf{I}_N$ in (16) and noting that $\sigma_J^2|\beta_m|^2\mathbf{w}_2^H\mathbf{s}_m\mathbf{s}_m^H\mathbf{w}_2 + \sigma_J^2 + \sigma_J^2(\beta_m^*\mathbf{s}_m^H\mathbf{w}_2 + \beta_m\mathbf{w}_2^H\mathbf{s}_m) = \sigma_J^2|1 + \beta_m\mathbf{w}_2^H\mathbf{s}_m|^2$, we have the following expression for the output power:

$$\begin{aligned} P_{\text{out}} &= \sigma_J^2\,|\beta_m|^2\,|\mathbf{w}_1^H\mathbf{s}_m|^2 \\ &\quad + \sigma_J^2\,|1 + \beta_m\mathbf{w}_2^H\mathbf{s}_m|^2 + \sigma_n^2(\mathbf{w}_1^H\mathbf{w}_1 + \mathbf{w}_2^H\mathbf{w}_2). \end{aligned} \tag{19}$$

In an ideal scenario, one would expect this expression to be free of jammer energy, that is, to achieve $\mathbf{w}_1^H\mathbf{s}_m \approx 0$ and $1 + \beta_m\mathbf{w}_2^H\mathbf{s}_m \approx 0$. The performance measure of the processor is generally indicated by the signal processing gain which is defined by the ratio $\text{SINR}_{\text{out}}/\text{SINR}_{\text{in}}$, where SINR_{in} is the input signal-to-interference ratio and SINR_{out} is the signal-to-interference ratio at the output. For the case of a mainlobe jammer plus single TSI path (with delay m), we have $\text{SINR}_{\text{in}} = |\alpha_t|^2/(\sigma_J^2(1 + |\beta_m|^2) + \sigma_n^2)$, $\text{SINR}_{\text{out}} = |\alpha_t|^2/P_{\text{out}}$, and the processing gain (P_G) is given by

$$P_G = \left(\frac{\sigma_n^2 + \sigma_J^2(1 + |\beta_m|^2)}{P_{\text{out}}}\right) = \left(\frac{\sigma_n^2}{P_{\text{out}}}\right)(1 + \text{Jnr}\,(1 + |\beta_m|^2)). \tag{20}$$

The performance of the processor can be measured by the quantity $\sigma_n^2/P_{\text{out}}$ which is the only algorithm-dependent part of the processing gain. Furthermore, this quantity is the processing gain in the absence of any interference sources (noise only detection) and it generally achieves the value N for most spatial beamformers. Therefore we may define the quantity

$$\tilde{P}_G = \frac{\sigma_n^2}{P_{\text{out}}} \tag{21}$$

as the processing gain for comparison of our selected algorithms. This measure is expected to achieve a value between 1 and N depending on the nature of the algorithm applied to null the mainlobe jammer and any other spatial interference sources. In order to obtain a quantitative figure for the processing gain, we may further analyse the array weights vector obtained above for the case of a mainlobe jammer and one TSI path as follows.

For $\mathbf{R}_1 = \sigma_J^2|\beta_m|^2\mathbf{s}_m\mathbf{s}_m^H + \sigma_n^2\mathbf{I}_N$, we have (using matrix inversion lemma [8])

$$\mathbf{R}_1^{-1} = \frac{1}{\sigma_n^2}\left[\mathbf{I}_N - \frac{(\sigma_J^2\,|\beta_m|^2\mathbf{s}_m\mathbf{s}_m^H)}{(\sigma_n^2 + N\,|\beta_m|^2\sigma_J^2)}\right], \tag{22}$$

$$\mathbf{R}_1^{-1}\mathbf{s}_t = \frac{1}{\sigma_n^2}\left[\mathbf{s}_t - \frac{(\sigma_J^2\,|\beta_m|^2\mathbf{s}_m\mathbf{s}_m^H\mathbf{s}_t)}{(\sigma_n^2 + N\,|\beta_m|^2\sigma_J^2)}\right], \tag{23}$$

$$\mathbf{R}_1^{-1}\mathbf{s}_m = \frac{\mathbf{s}_m}{\sigma_n^2 + N\,|\beta_m|^2\sigma_J^2}, \tag{24}$$

$$\mathbf{s}_m^H\mathbf{R}_1^{-1}\mathbf{s}_m = \frac{N}{\sigma_n^2 + N\,|\beta_m|^2\sigma_J^2}, \tag{25}$$

$$\mathbf{s}_m^H\mathbf{R}_1^{-1}\mathbf{s}_t = \frac{\mathbf{s}_m^H\mathbf{s}_t}{\sigma_n^2 + N\,|\beta_m|^2\sigma_J^2}, \tag{26}$$

and (for $N|\beta_m|^2\,\text{Jnr} \gg 1$)

$$\begin{aligned} \mathbf{s}_t^H\mathbf{R}_1^{-1}\mathbf{s}_t &= \frac{1}{\sigma_n^2}\left[N - \frac{(\sigma_J^2\,|\beta_m|^2\,|\mathbf{s}_t^H\mathbf{s}_m|^2)}{(\sigma_n^2 + N\,|\beta_m|^2\sigma_J^2)}\right] \\ &= \frac{N}{\sigma_n^2}\left[1 - \frac{|\mathbf{s}_t^H\mathbf{s}_m|^2\,|\beta_m|^2\,\text{Jnr}}{N(1 + N\,|\beta_m|^2\,\text{Jnr})}\right] \\ &\approx \frac{N}{\sigma_n^2}\left(1 - \frac{|\mathbf{s}_t^H\mathbf{s}_m|^2}{N^2}\right) \approx \frac{N}{\sigma_n^2}. \end{aligned} \tag{27}$$

The assumption made in the last expression (i.e., $|\mathbf{s}_t^H\mathbf{s}_m|/N^2 \approx 0$) is very accurate when the signals are not closely

spaced. The other assumption made throughout this study is that the mainlobe jammer is above the noise floor (i.e., Jnr > 1). In this case, we need at least $|\beta_m|^2 \gg 1/N$ (or equivalently $N|\beta|^2\,\mathrm{Jnr} \gg 1$) in order to achieve any processing gain as seen later. We will also see that when $|\beta_m|^2$ is closer to the lower bound of $1/N$, we do not achieve any processing gain. Therefore, we would like to investigate the two cases $|\beta_m|^2 \gg 1/N$ and $|\beta_m|^2 \ll 1/N$ simultaneously. The value of the expression (27) for $|\beta_m|^2 \ll 1/N$ (or $N|\beta_m|^2\,\mathrm{Jnr} \ll 1$) can be simplified as follows:

$$\begin{aligned}\mathbf{s}_t^H\mathbf{R}_1^{-1}\mathbf{s}_t &\approx \frac{N}{\sigma_n^2}\left[1-\frac{|\mathbf{s}_t^H\mathbf{s}_m|^2|\beta_m|^2\,\mathrm{Jnr}}{N}\right]\\ &\approx \frac{N}{\sigma_n^2}\left[1-\frac{|\mathbf{s}_t^H\mathbf{s}_m|^2(N|\beta_m|^2)\,\mathrm{Jnr}}{N^2}\right]\\ &\approx \frac{N}{\sigma_n^2}.\end{aligned} \tag{28}$$

Furthermore, applying the above formula and (24) in (17) we can see that

$$\begin{aligned}|\mathbf{w}_1^H\mathbf{s}_m|^2 &= \left|\frac{\mathbf{s}_t^H\mathbf{R}_1^{-1}\mathbf{s}_m}{\mathbf{s}_t^H\mathbf{R}_1^{-1}\mathbf{s}_t}\right|^2\\ &= \left|\frac{\mathbf{s}_t^H}{\mathbf{s}_t^H\mathbf{R}_1^{-1}\mathbf{s}_t}\cdot\frac{\mathbf{s}_m}{(\sigma_n^2+N|\beta_m|^2\sigma_f^2)}\right|^2\\ &\approx \frac{(|\mathbf{s}_t^H\mathbf{s}_m|^2/N^2)}{(1+N|\beta_m|^2\,\mathrm{Jnr})^2}\approx 0.\end{aligned} \tag{29}$$

This expression shows how closely we have achieved the orthogonality requirement expected above. It is reasonable to assume that $\mathbf{w}_1^H\mathbf{s}_m \approx 0$ (or equivalently $|\mathbf{s}_t^H\mathbf{s}_M|^2/N^2 \approx 0$) for all possible positive values of $N|\beta_m|^2$. We may now investigate the second and third terms as the dominant terms at the processor output in (19). The approximate expressions for these two terms can be derived using (22)–(27) (see appendix) as

$$|1+\beta_m\mathbf{w}_2^H\mathbf{s}_m|^2 \approx \begin{cases}\dfrac{1}{(N|\beta_m|^2\,\mathrm{Jnr})^2} & \text{for } N|\beta_m|^2\,\mathrm{Jnr}\gg 1,\\ 1-2N|\beta_m|^2\,\mathrm{Jnr} & \text{for } N|\beta_m|^2\,\mathrm{Jnr}\ll 1,\end{cases}$$

$$\sigma_n^2\|\mathbf{w}\|^2 = \begin{cases}\sigma_n^2\left(\dfrac{1}{N}+\dfrac{1}{N|\beta_m|^2}\right) & \text{for } N|\beta_m|^2\,\mathrm{Jnr}\gg 1,\\ \sigma_n^2\left(\dfrac{1}{N}+N|\beta_m|^2\,\mathrm{Jnr}^2\right) & \text{for } N|\beta_m|^2\,\mathrm{Jnr}\ll 1.\end{cases} \tag{30}$$

Substituting (30) in (19) we can evaluate $P_{\mathrm{out}}/\sigma_n^2$ as

$$\frac{P_{\mathrm{out}}}{\sigma_n^2} \approx \begin{cases}\left(\dfrac{1}{N}+\dfrac{1}{N|\beta_m|^2}\right)+\dfrac{1}{N^2|\beta_m|^4\,\mathrm{Jnr}} & \text{for } N|\beta_m|^2\,\mathrm{Jnr}\gg 1,\\ \dfrac{1}{N}+\mathrm{Jnr}-N|\beta_m|^2\,\mathrm{Jnr}^2 & \text{for } N|\beta_m|^2\,\mathrm{Jnr}\ll 1,\end{cases} \tag{31}$$

which can be approximated to

$$\frac{P_{\mathrm{out}}}{\sigma_n^2} \approx \begin{cases}\dfrac{N|\beta_m|^4\,\mathrm{Jnr}+N|\beta_m|^2\,\mathrm{Jnr}+1}{N^2|\beta_m|^4\,\mathrm{Jnr}} & \text{for } N|\beta_m|^2\,\mathrm{Jnr}\gg 1,\\ \dfrac{1}{N}+\mathrm{Jnr} & \text{for } N|\beta_m|^2\,\mathrm{Jnr}\ll 1.\end{cases} \tag{32}$$

As a result, we have the processing gain (substituting $N|\beta_m|^4\,\mathrm{Jnr}+N|\beta_m|^2\,\mathrm{Jnr}+1 \approx N|\beta_m|^4\,\mathrm{Jnr}+N|\beta_m|^2\,\mathrm{Jnr}$ in the above expression for $N|\beta_m|^2\,\mathrm{Jnr}\gg 1$ case)

$$\tilde{P}_G = \frac{\sigma_n^2}{P_{\mathrm{out}}} \approx \begin{cases}\dfrac{N|\beta_m|^2}{1+|\beta_m|^2}, & N|\beta_m|^2\,\mathrm{Jnr}\gg 1,\\ \dfrac{N}{1+N\,\mathrm{Jnr}-N^2|\beta_m|^2\,\mathrm{Jnr}^2}, & N|\beta_m|^2\,\mathrm{Jnr}\ll 1.\end{cases} \tag{33}$$

Whenever the mainlobe jammer power is above the noise floor, the algorithm can achieve greater than one processing gain only if $|\beta_m|^2 > 1/N$ and the value of this gain falls far shorter than N. The maximum possible value for $N|\beta_m|^2/(1+|\beta_m|^2)$ is around $N/2$ when $|\beta_m|^2 = 1$. For $N|\beta_m|^2\,\mathrm{Jnr} \ll 1$, $\tilde{P}_G \approx 1/\mathrm{Jnr} < 1$. As seen later in the simulation section, the conclusions drawn here do not change significantly when one or two sidelobe interferers are considered. The only difference is that (19) will have additional terms due to sidelobe jammers and other TSI paths. The added terms in (19) are of the form $\sigma_k^2|\mathbf{w}_1^H\mathbf{s}_k|^2$ $(k = 1, 2, \ldots)$ and they satisfy the orthogonality requirement in a very similar manner.

5. TSI FINDING

Now consider the following dimensionless measure:

$$\begin{aligned}T_S(m) &= \left\{(\mathbf{w}^H\mathbf{R}\mathbf{w})^{-1}(\mathbf{s}_t^H\mathbf{R}_x^{-1}\mathbf{s}_t)^{-1}-1\right\}\\ &= \frac{(\mathbf{s}_t^H\mathbf{R}_x^{-1}\mathbf{s}_t)^{-1}}{P_{\mathrm{out}}}-1,\end{aligned} \tag{34}$$

where m refers to the "guessed" time delay used in forming the space fast-time processor as explained previously, $\mathbf{w}$ is the array's $2N \times 1$ space fast-time weights vector obtained via the direct MPDR filter (11) which optimises the power $\mathbf{w}^H\mathbf{R}\mathbf{w}$ subject to the constraints $\mathbf{w}^H(\mathbf{s}_t^T, \mathbf{o}^T)^T = 1$ and $\mathbf{w}^H(\mathbf{o}^T, \mathbf{s}_t^T)^T = 0$. $\mathbf{R}_x$ is the $N \times N$ measured spatial covariance matrix. By denoting the value of $T_S(m)$ for $m = n_k$ (for some k) by $T_S(m)_{m=n_k}$ and noting that $P_{\mathrm{out}} = \mathbf{w}^H\mathbf{R}\mathbf{w}$, we can use the earlier result (33) to show that

$$T_s(m)_{m=n_k} \approx (\mathbf{s}_t^H\mathbf{R}_x^{-1}\mathbf{s}_t)^{-1}\frac{N|\beta|^2}{\sigma_n^2(1+|\beta|^2)}-1 \quad \text{for } N|\beta|^2\,\mathrm{Jnr}\gg 1, \tag{35}$$

where β represents a reflectivity coefficient corresponding to any of the TSI paths (at least one) available. In order to further simplify the above expression, we need to use the following matrix inversion lemma.

Lemma 1. *Suppose the square matrix* $\mathbf{A}$ *is added to an additional dyad term* $\mathbf{u}\mathbf{u}^H$*, where* $\mathbf{u}$ *is a column vector, then the inversion of the new matrix is given by (e.g., [8])*

$$\left(\mathbf{A}+\mathbf{u}\mathbf{u}^H\right)^{-1}=\mathbf{A}^{-1}-\frac{\mathbf{A}^{-1}\mathbf{u}\mathbf{u}^H\mathbf{A}^{-1}}{1+\mathbf{u}^H\mathbf{A}^{-1}\mathbf{u}}. \tag{36}$$

By definition we have $\mathbf{R}_x=\sigma_f^2\mathbf{s}_t\mathbf{s}_t^H+\mathbf{R}_1$, where

$$\mathbf{R}_1=\sigma_f^2\left|\beta_m\right|^2\mathbf{s}_m\mathbf{s}_m^H+\sigma_n^2\mathbf{I}_N+\left(\sum_{k=1}^{m-1}\sigma_f^2\left|\beta_k\right|^2\mathbf{s}_k\mathbf{s}_k^H+\sum_{k=m+1}^{K}\sigma_f^2\left|\beta_k\right|^2\mathbf{s}_k\mathbf{s}_k^H+\sum_{k=1}^{Q}\hat{\sigma}_f^2\hat{\mathbf{s}}_k\hat{\mathbf{s}}_k^H\right). \tag{37}$$

Applying the above lemma, we have the following identity:

$$\mathbf{R}_x^{-1}=\mathbf{R}_1^{-1}-\frac{\sigma_f^2\left(\mathbf{R}_1^{-1}\mathbf{s}_t\mathbf{s}_t^H\mathbf{R}_1^{-1}\right)}{1+\sigma_f^2\left(\mathbf{s}_t^H\mathbf{R}_1^{-1}\mathbf{s}_t\right)}. \tag{38}$$

This leads to the expression

$$\begin{aligned}\mathbf{s}_t^H\mathbf{R}_x^{-1}\mathbf{s}_t&=\mathbf{s}_t^H\mathbf{R}_1^{-1}\mathbf{s}_t-\frac{\sigma_f^2\left(\mathbf{s}_t^H\mathbf{R}_1^{-1}\mathbf{s}_t\mathbf{s}_t^H\mathbf{R}_1^{-1}\mathbf{s}_t\right)}{1+\sigma_f^2\left(\mathbf{s}_t^H\mathbf{R}_1^{-1}\mathbf{s}_t\right)}\\&=\frac{\mathbf{s}_t^H\mathbf{R}_1^{-1}\mathbf{s}_t}{1+\sigma_f^2\left(\mathbf{s}_t^H\mathbf{R}_1^{-1}\mathbf{s}_t\right)},\end{aligned} \tag{39}$$

$$\left(\mathbf{s}_t^H\mathbf{R}_x^{-1}\mathbf{s}_t\right)^{-1}=\sigma_f^2+\left(\mathbf{s}_t^H\mathbf{R}_1^{-1}\mathbf{s}_t\right)^{-1}.$$

Substituting (39) in (35), we have

$$T_S(m)_{m=n_k}=\begin{cases}\left(\sigma_f^2+\left(\mathbf{s}_t^H\mathbf{R}_1^{-1}\mathbf{s}_t\right)^{-1}\right)\dfrac{N|\beta|^2}{\sigma_n^2(1+|\beta|^2)}-1, & N|\beta|^2\,\mathrm{Jnr}\gg 1,\\ \left(\sigma_f^2+\left(\mathbf{s}_t^H\mathbf{R}_1^{-1}\mathbf{s}_t\right)^{-1}\right)\dfrac{N}{\sigma_n^2(1+N\,\mathrm{Jnr}-N^2|\beta|^2\,\mathrm{Jnr}^2)}-1, & N|\beta|^2\,\mathrm{Jnr}\ll 1.\end{cases} \tag{40}$$

For the case of a mainlobe jammer and a single TSI path we have shown that $(\mathbf{s}_t^H\mathbf{R}_1^{-1}\mathbf{s}_t)\approx N/\sigma_n^2$ for $N|\beta_m|^2\,\mathrm{Jnr}\ll 1$ and $N|\beta_m|^2\,\mathrm{Jnr}\gg 1$. As a result we have for $N|\beta_m|^2\,\mathrm{Jnr}\gg 1$

$$\begin{aligned}T_S(m)_{m=n_k}&=\left(\sigma_f^2+\frac{\sigma_n^2}{N}\right)\frac{N|\beta|^2}{\sigma_n^2(1+|\beta|^2)}-1\\&\approx\frac{N|\beta|^2\,\mathrm{Jnr}-1}{(1+|\beta|^2)}\\&\approx N|\beta|^2\,\mathrm{Jnr},\end{aligned} \tag{41}$$

and for $N|\beta|^2\,\mathrm{Jnr}\ll 1$

$$\begin{aligned}T_S(m)_{m=n_k}&=\frac{(\sigma_f^2+\sigma_n^2/N)}{P_{\mathrm{out}}}-1\\&=\frac{N(\sigma_f^2+\sigma_n^2/N)}{\sigma_n^2(1+N\,\mathrm{Jnr}-N^2|\beta|^2\,\mathrm{Jnr}^2)}-1\\&\approx\frac{N^2|\beta|^2\,\mathrm{Jnr}^2}{(1+N\,\mathrm{Jnr}\,(1-N|\beta|^2\,\mathrm{Jnr}))}\\&\approx\frac{N^2|\beta|^2\,\mathrm{Jnr}^2}{(1+N\,\mathrm{Jnr})}\approx N|\beta|^2\,\mathrm{Jnr}.\end{aligned} \tag{42}$$

The interesting observation made here is that the quantity $T_S(m)_{m=n_k}$ represents a large value, which is proportional to N Jnr when the selected delay (m) matches with one of the path delays (n_k) regardless of how minute the value of $|\beta|^2$ is. It will now be interesting to evaluate the value of $T_S(m)$ for a mismatch (i.e., $T_S(m)_{m\neq n_k}$). Let us consider the case where $m\neq n_k$ for any k. Then (13) has the following format:

$$\mathbf{R}=\begin{pmatrix}\sigma_f^2\mathbf{s}_t\mathbf{s}_t^H+\mathbf{R}_1 & 0\\ 0 & \sigma_f^2\mathbf{s}_t\mathbf{s}_t^H+\mathbf{R}_1\end{pmatrix}=\begin{pmatrix}\mathbf{R}_x & 0\\ 0 & \mathbf{R}_x\end{pmatrix}. \tag{43}$$

(Note that in this case, the signal subspace consists of the base vectors $(\mathbf{s}_t^T,\mathbf{o}^T)^T$, $(\mathbf{o}^T,\mathbf{s}_t^T)^T$, $(\mathbf{s}_m^T,\mathbf{o}^T)^T$, $(\mathbf{o}^T,\mathbf{s}_m^T)^T$, and other linearly independent vectors such as $(\mathbf{o}^T,\mathbf{s}_k^T)^T$, $(\mathbf{s}_k^T,\mathbf{o}^T)^T$, $k=1,2,\ldots,K$, arising from other TSI paths and $(\mathbf{o}^T,\hat{\mathbf{s}}_k^T)^T$, $(\hat{\mathbf{s}}_k^T,\mathbf{o}^T)^T$, $k=1,2,\ldots,Q$, due to other sidelobe jammers.)

The output power at the processor is given by

$$\begin{aligned}\mathbf{w}^H\mathbf{R}\mathbf{w}=\mathbf{w}_1^H\mathbf{R}_1\mathbf{w}_1+\mathbf{w}_2^H\mathbf{R}_1\mathbf{w}_2\\+\sigma_f^2\mathbf{w}_1^H\mathbf{s}_t\mathbf{s}_t^H\mathbf{w}_1^{+}\sigma_f^2\mathbf{w}_2^H\mathbf{s}_t\mathbf{s}_t^H\mathbf{w}_2.\end{aligned} \tag{44}$$

The minimisation of power subject to the same constraints (as applied to (15)), leads to the following solution:

$$\begin{aligned}\mathbf{w}_1&=\frac{\mathbf{R}_1^{-1}\mathbf{s}_t}{\left(\mathbf{s}_t^H\mathbf{R}_1^{-1}\mathbf{s}_t\right)},\\ \mathbf{w}_2&=\mathbf{o}_{N\times 1}.\end{aligned} \tag{45}$$

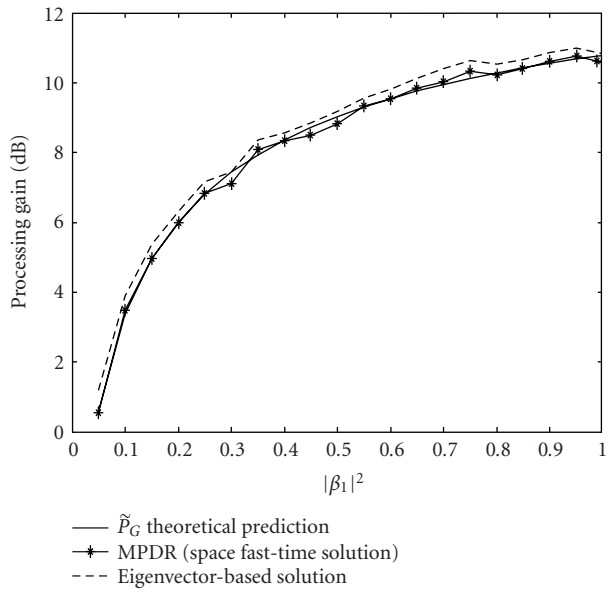

Figure 1: Processing gain for two solutions versus the theoretical prediction.

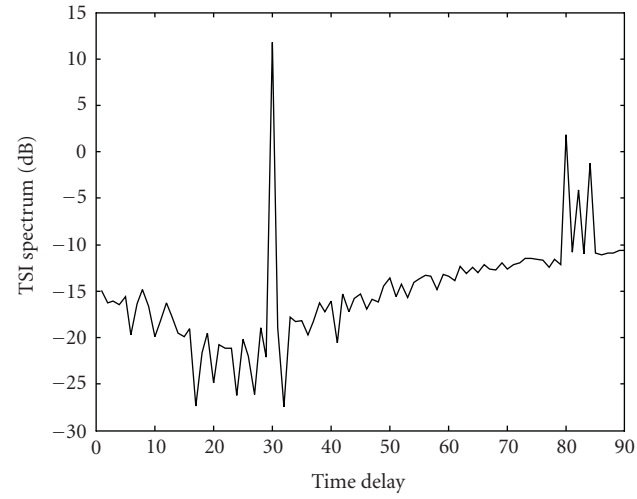

Figure 2: TSI spectrum representing 4 TSI arrivals where 30, 80, 82, and 84 are the time delays and the associated directions of arrivals are $(5^\circ, 0^\circ)$, $(-30^\circ, 0^\circ)$, $(-32^\circ, 0^\circ)$, and $(-34^\circ, 0^\circ)$. The corresponding reflectivities are $|\beta_1|^2 = 1/4$, $|\beta_2|^2 = 1/40$, $|\beta_3|^2 = 1/80$, and $|\beta_4|^2 = 1/90$, respectively.

In this case we have the following expression for the processor output power:

$$\begin{aligned} P_{\text{out}} &= \mathbf{w}^H \mathbf{R}\mathbf{w} \\ &= \mathbf{w}_1^H \mathbf{R}\mathbf{w}_1 + \sigma_f^2 \mathbf{w}_1^H \mathbf{s}_t \mathbf{s}_t^H \mathbf{w}_1 \\ &= \left(\mathbf{s}_t^H \mathbf{R}_1^{-1} \mathbf{s}_t\right)^{-1} + \sigma_f^2. \end{aligned} \tag{46}$$

Substituting this expression in (34) leads to

$$T_S(m)_{m \neq n_k} = \frac{\left(\mathbf{s}_t^H \mathbf{R}_x^{-1} \mathbf{s}_t\right)^{-1}}{\left(\mathbf{s}_t^H \mathbf{R}_1^{-1} \mathbf{s}_t\right)^{-1} + \sigma_f^2} - 1 \equiv 0 \tag{47}$$

using (39). The most important fact here is that we do not have to assume the simple case of a mainlobe jammer and one TSI path to prove that this quantity is zero. The TSI finder spectrum has the following properties:

$$T_S(m) = \begin{cases} N|\beta|^2 \,\text{Jnr}, & m = n_k, \\ 0, & m \neq n_k. \end{cases} \tag{48}$$

The TSI spectrum has an almost infinite processing gain when inverted (at least in theory), and is able to detect extremely small TSI power levels which will be shown by simulation in Section 6.

6. SIMULATION

In this section we illustrate several examples using simulated data. In the first example we have considered 800 range samples for an airborne linear equispaced array of 24 elements with half-wavelength spacings. The transmitter is assumed to transmit a single pulse towards a target in the 10th range cell where $(\phi_t, \theta_t) = (0^\circ, 0^\circ)$. It is assumed that the transmitter does not illuminate the ground with sufficient energy to consider the clutter return. However, a mainlobe jammer is present in the target direction which is 10 dB above noise floor (Jnr $= 10\,\text{dB}, \sigma_n^2 = 1$). Target power level at the receiver is 0 dB. Mainlobe jammer is assumed to produce 4 TSI paths where $(5^\circ, 0^\circ)$, $(-30^\circ, 0^\circ)$, $(-32^\circ, 0^\circ)$, $(-34^\circ, 0^\circ)$ represent the directions of arrivals, and the associated path delays are 30, 80, 82, 84, respectively. This represents a scenario where the last three arrivals occur in a cluster. The associated power ratios are given by $|\beta_k|^2$ $(k = 1, 2, 3, 4)$, where $|\beta_1|^2$ is treated as a variable and $|\beta_2|^2 = 1/40$, $|\beta_3|^2 = 1/80$, $|\beta_4|^2 = 1/90$ are fixed. The estimated signal processing gain using simulated output data $(= \sigma_n^2/(\mathbf{w}^H \mathbf{R}\mathbf{w}))$ and the theoretical prediction $\tilde{P}_G \approx N|\beta_1|^2/(1 + |\beta_1|^2)$ of (33) is illustrated in Figure 1. Highest predicted value for the processing gain $(\approx 10\log_{10}(N/2))$ is achieved when the reflectivity coefficient $|\beta_1|^2$ is close to 1.0 as predicted by the theory. The processing gain may further be reduced when the sidelobe jammers are present. The TSI spectrum $(10\log_{10}(T_s(m)))$ always picks up the correct time lags. A typical TSI spectrum when $|\beta_1|^2 = 0.25$ is illustrated in Figure 2. Figure 3 shows the MPDR-based space fast-time processor outputs for the first 100 range cells. Furthermore, the same plot displays the results of the usual spatial beamformer where we simply invert the $N \times N$ measured covariance matrix to obtain the array weights. In this case, as predicted, the processor output reproduces the stream of random numbers used in simulating the mainlobe jammer (i.e., $j(r)$) where $E\{|j(r)|^2\} = 10\,\text{dB}$.

In a second example, we would like to simulate a more realistic TSI scenario by assuming that all TSI paths are reflected off the ground by changing their directions of arrival from the set $(5^\circ, 0^\circ)$, $(-30^\circ, 0^\circ)$, $(-32^\circ, 0^\circ)$, $(-34^\circ, 0^\circ)$ to $(5^\circ, -10^\circ)$, $(-30^\circ, -15^\circ)$, $(-32^\circ, -20^\circ)$, $(-34^\circ, -25^\circ)$. The mainlobe jammer power is increased from 10 dB to 30 dB.

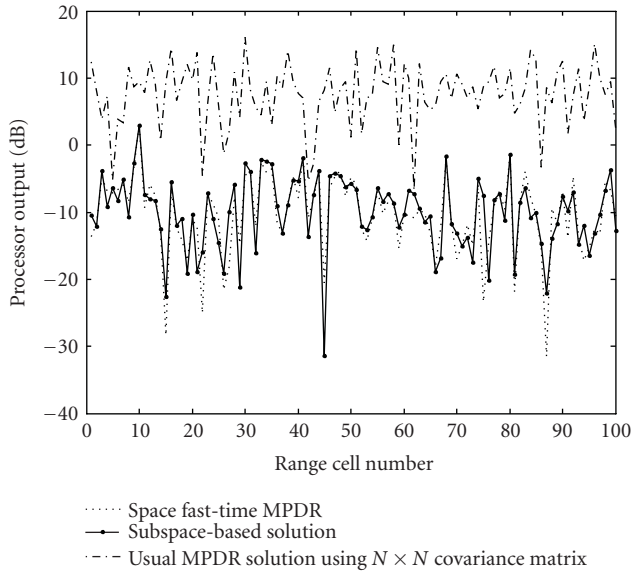

FIGURE 3: The processor output for two methods and the usual spatial beamformer in the first 100 range cells. The target resides in the 10th-range cell.

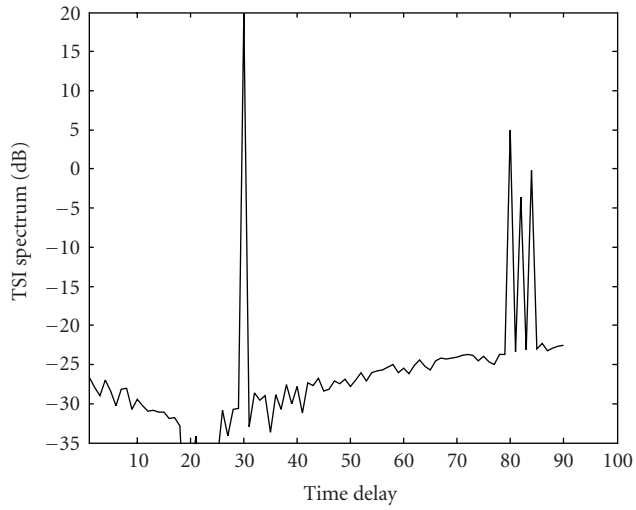

FIGURE 4: Improved TSI spectrum using 800×16 range samples. Correct delay points are detected at 30, 80, 82, and 84.

Furthermore, (1) is altered to generate 16 coherent pulses using

$$\mathbf{x}_m(r) = \alpha_t \delta(r - r_0)\mathbf{s}(\phi_t, \theta_t) \exp(j2\pi f_d mT) + j_m(r)\mathbf{s}(\phi_t, \theta_t) + \sum_{k=1}^{k=K} \beta_k j_m(r - n_k)\mathbf{s}(\phi_k, \theta_k) + \boldsymbol{\varepsilon}_{r,m}, \tag{49}$$

where $m = 0, 1, 2, \ldots, M-1$ represent $M(= 16)$ coherent pulses, $j_m(r)$ is a random function, $\boldsymbol{\varepsilon}_{m,t}$ is a $N \times 1$ column vector containing independent and identical Gaussian random numbers with unit variance and zero mean, T is the pulse repetition interval, and f_d is the target Doppler. $T = 10^{-4}$ and $f_d = 12/(MT)$ are the values used in the simulation. All other parameters remain as in the previous example. In this example the plot of the TSI finder has been further improved due to the fact that 16 times more data was available when averaging the outer products to form the TSI finder. This is clearly seen in Figure 4. The STAP processor output is passed through a digital FFT processor to achieve further processing gain of $M(= 12\,\text{dB})$ as seen in Figure 5. The target in the 10th range cell has been enhanced considerably in comparison to the single pulse output shown earlier.

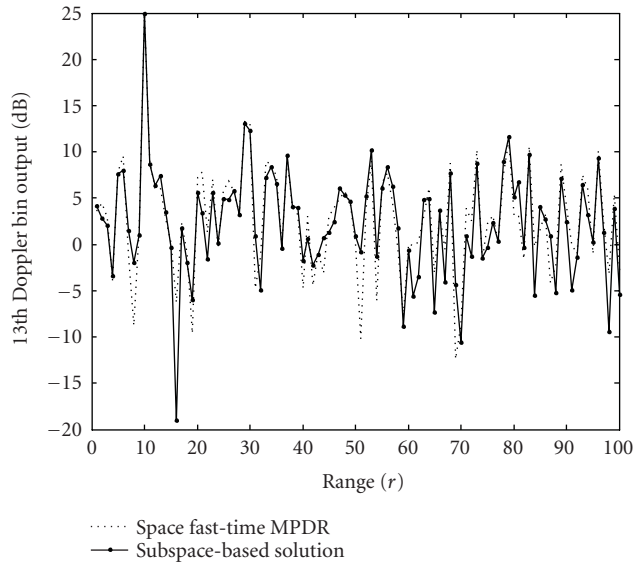

FIGURE 5: Output of the space fast-time adaptive processor (MPDR) for the 13th Doppler bin as a function of range for the first 100 range cells.

6.1. The effect of taps

As we interrogate the rth range cell for targets in the presence of a mainlobe jammer, we would like the proposed TSI finder to determine the exact time delay so as to form the $2N \times 1$ space fast-time data snapshot at each range. For the example in Figure 4, one would use $(r + 30)$th-range cell data to form the space fast-time snapshot. However, in practice, we may use several range returns to form the STAP processor. For instance, it is advisable to form a $4N \times 1$ (or larger) snapshot by incorporating r, $r + 29$, $r + 30$, $r + 31$. This will increase the order of the space fast-time covariance matrix to $4N \times 4N$ at the STAP processor, and hence the computational complexity by several orders (approximately 8 times), but it secures the inclusion of the TSI into the STAP processor. In order to demonstrate this invariance to the number of taps being used at the processor (provided that at least one TSI is included in the selected set), we have

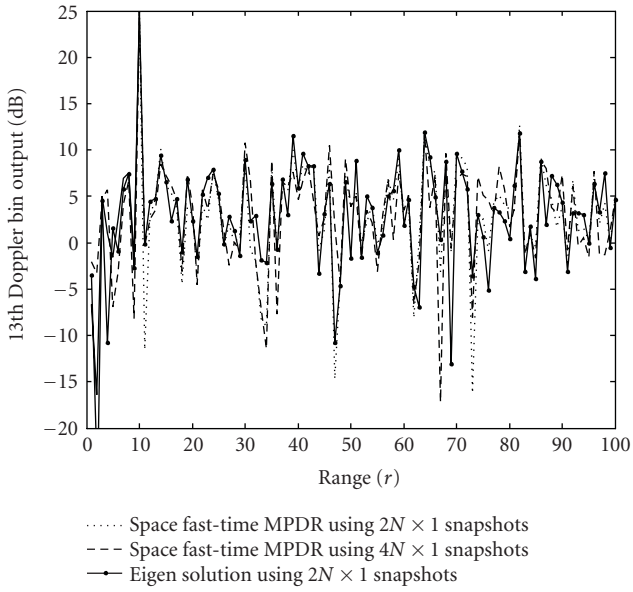

FIGURE 6: Output of the space fast-time adaptive processor (MPDR) for the 13th Doppler bin as a function of range.

repeated the result in Figure 5 with 2 taps and 4 taps. The outputs are displayed in Figure 6 which clearly shows that the number of taps are not relevant. In fact this result can be further verified theoretically as well. It should also be noted that when higher-order snapshots are formed at the processor, then one would obtain the corresponding $4N \times 1$ space fast-time weights vector by minimising $\mathbf{w}^H\mathbf{R}\mathbf{w}$ subject to $\mathbf{w}^H(\mathbf{s}_t^T, \mathbf{o}^T, \mathbf{o}^T, \mathbf{o}^T)^T = 1$, $\mathbf{w}^H(\mathbf{o}^T, \mathbf{s}_t^T, \mathbf{o}^T, \mathbf{o}^T)^T = 0$, $\mathbf{w}^H(\mathbf{o}^T, \mathbf{o}^T, \mathbf{s}_t^T, \mathbf{o}^T)^T = 0$, $\mathbf{w}^H(\mathbf{o}^T, \mathbf{o}^T, \mathbf{o}^T, \mathbf{s}_t^T)^T = 0$. A similar argument holds for the subspace-based solution as well.

7. APPLICATION TO CLUTTER

In airborne look down applications where the clutter return is significant, we need to apply the space fast-time slow-time adaptive processing which is equivalent to stacking two conventional STAP (i.e., space slow-time adaptive processors) processors provided one has the knowledge of the TSI finder to select the best fast-time delay. The TSI finder described in this study uses the $2N \times 2N$ space fast-time covariance matrix with jammers only. For HPRF radar one can convert the data into frequency domain and discard the Doppler bins that contain clutter energy. Using the data in the frequency domain corresponding to all the clutter-free Doppler bins, one can estimate the jammer-only covariance matrix very accurately [9] and form the TSI finder as in (34). For LPRF and MPRF radars, the computation of the clutter-free covariance matrix is not always straightforward and these complexities are beyond the scope of this study.

8. CONCLUSION

The TSI finder introduced in this study is a highly accurate process to find very small power levels and associated time delays by forming a series of $2N \times 2N$ covariance matrices. Finding the time delay corresponding to the highest point of the TSI spectrum almost always provides the best lag, which corresponds to the most powerful TSI available. However the achievable signal processing gain of the final output is determined by the power level of this TSI path. The eigenvector-based approach seems to perform marginally better than MPDR but at a higher computational cost (80% or more). The advantage of the use of the subspace technique is that it produces around 0.4 dB additional processing gain in almost all the cases simulated (as predicted in Figure 1). By formulating a suitable threshold detector on the TSI finder we can automate the process of attempting to null mainlobe jammer whenever a sufficiently powerful TSI is available. At all other times the process does not have to go into the space fast-time mode unnecessarily.

APPENDIX

From (18), we have

$$\begin{aligned}
&\beta_m \mathbf{w}_2^H \mathbf{s}_m \\
&\quad = \beta_m \left[-\beta_m \sigma_J^2 \mathbf{R}_1^{-1}\mathbf{s}_m + \beta_m \sigma_J^2 \left(\frac{\mathbf{s}_t^H \mathbf{R}_1^{-1}\mathbf{s}_m}{\mathbf{s}_t^H \mathbf{R}_1^{-1}\mathbf{s}_t} \right) \mathbf{R}_1^{-1}\mathbf{s}_t \right]^H \mathbf{s}_m \\
&\quad = -|\beta_m|^2 \sigma_J^2 \mathbf{s}_m^H \mathbf{R}_1^{-1}\mathbf{s}_m + \frac{|\beta_m|^2 \sigma_J^2 |\mathbf{s}_t^H \mathbf{R}_1^{-1}\mathbf{s}_m|^2}{\mathbf{s}_t^H \mathbf{R}_1^{-1}\mathbf{s}_t}.
\end{aligned} \tag{A.1}$$

Now further simplification of (A.1) using (25) leads to

$$\begin{aligned}
1 + \beta_m \mathbf{w}_2^H \mathbf{s}_m &= 1 - \frac{|\beta_m|^2 \sigma_J^2 N}{\sigma_n^2 + N|\beta_m|^2 \sigma_J^2} + \frac{|\beta_m|^2 \sigma_J^2 |\mathbf{s}_t^H \mathbf{R}_1^{-1}\mathbf{s}_m|^2}{\mathbf{s}_t^H \mathbf{R}_1^{-1}\mathbf{s}_t} \\
&= \frac{\sigma_n^2}{\sigma_n^2 + N|\beta_m|^2 \sigma_J^2} + \frac{|\beta_m|^2 \sigma_J^2 |\mathbf{s}_t^H \mathbf{R}_1^{-1}\mathbf{s}_m|^2}{\mathbf{s}_t^H \mathbf{R}_1^{-1}\mathbf{s}_t},
\end{aligned} \tag{A.2}$$

where the second term on the right-hand side can be simplified using (26), (27) and finally assuming $N|\beta_m|^2\,\mathrm{Jnr} \gg 1$ (i.e., $1 + N|\beta_m|^2\,\mathrm{Jnr} \approx N|\beta_m|^2\,\mathrm{Jnr}$) as follows:

$$\begin{aligned}
&\frac{|\beta_m|^2 \sigma_J^2 |\mathbf{s}_t^H \mathbf{R}_1^{-1}\mathbf{s}_m|^2}{\mathbf{s}_t^H \mathbf{R}_1^{-1}\mathbf{s}_t} \\
&\quad = \frac{|\beta_m|^2 \sigma_J^2 |\mathbf{s}_m^H \mathbf{s}_t|^2}{(N/\sigma_n^2)(\sigma_n^2 + N|\beta_m|^2 \sigma_J^2)^2} = \frac{|\beta_m|^2 |\mathbf{s}_m^H \mathbf{s}_t|^2\,\mathrm{Jnr}}{N(1 + N|\beta_m|^2\,\mathrm{Jnr})^2} \\
&\quad \approx \frac{|\mathbf{s}_m^H \mathbf{s}_t|^2/N^2}{(N|\beta_m|^2\,\mathrm{Jnr})} \approx 0 \quad \text{for } N|\beta_m|^2\,\mathrm{Jnr} \gg 1,
\end{aligned}$$

$$\begin{aligned}
&\frac{|\beta_m|^2 \sigma_J^2 |\mathbf{s}_t^H \mathbf{R}_1^{-1}\mathbf{s}_m|^2}{\mathbf{s}_t^H \mathbf{R}_1^{-1}\mathbf{s}_t} \\
&\quad = \frac{|\beta_m|^2 |\mathbf{s}_m^H \mathbf{s}_t|^2\,\mathrm{Jnr}}{N(1 + N|\beta_m|^2\,\mathrm{Jnr})^2} \approx \frac{|\beta_m|^2 |\mathbf{s}_m^H \mathbf{s}_t|^2\,\mathrm{Jnr}}{N} \\
&\quad = (N|\beta_m|^2\,\mathrm{Jnr}) \frac{|\mathbf{s}_m^H \mathbf{s}_t|^2}{N^2} \approx 0 \quad \text{for } N|\beta_m|^2\,\mathrm{Jnr} \ll 1.
\end{aligned} \tag{A.3}$$

As a result we have

$$|1+\beta_m \mathbf{w}_2^H \mathbf{s}_s|^2 \approx \begin{cases} \dfrac{1}{(N|\beta_m|^2\,\mathrm{Jnr})^2} & \text{for } N|\beta_m|^2\,\mathrm{Jnr} \gg 1, \\ 1-2N|\beta_m|^2\,\mathrm{Jnr} & \text{for } N|\beta_m|^2\,\mathrm{Jnr} \ll 1. \end{cases} \tag{A.4}$$

The final term of the power output at the processor, that is, $\sigma_n^2(\mathbf{w}_1^H\mathbf{w}_1 + \mathbf{w}_2^H\mathbf{w}_2) = \sigma_n^2\|\mathbf{w}\|^2$ can be approximated as follows.

Using (17) and (27), we have

$$\begin{aligned} \mathbf{w}_1^H\mathbf{w}_1 &= \left(\frac{\mathbf{R}_1^{-1}\mathbf{s}_t}{\mathbf{s}_t^H\mathbf{R}_1^{-1}\mathbf{s}_t}\right)^H \left(\frac{\mathbf{R}_1^{-1}\mathbf{s}_t}{\mathbf{s}_t^H\mathbf{R}_1^{-1}\mathbf{s}_t}\right) \\ &\approx \frac{\sigma_n^4}{N^2}(\mathbf{R}_1^{-1}\mathbf{s}_t)^H(\mathbf{R}_1^{-1}\mathbf{s}_t). \end{aligned} \tag{A.5}$$

Substituting (23) and $\mathbf{s}_t^H\mathbf{s}_t = N$ in the above expression and noting that $1 + N|\beta_m|^2\,\mathrm{Jnr} \approx N|\beta_m|^2\,\mathrm{Jnr}$ (i.e., $N|\beta_m|^2\,\mathrm{Jnr} \gg 1$), we get

$$\begin{aligned} &\mathbf{w}_1^H\mathbf{w}_1 \\ &\approx \frac{\sigma_n^4}{N^2}\cdot\frac{1}{\sigma_n^4}\left\{N - \frac{2\sigma_J^2|\beta_m|^2|\mathbf{s}_t^H\mathbf{s}_m|^2}{(\sigma_n^2+N|\beta_m|^2\sigma_J^2)} + \frac{\sigma_J^4|\beta_m|^4|\mathbf{s}_t^H\mathbf{s}_m|^2 N}{(\sigma_n^2+N|\beta_m|^2\sigma_J^2)^2}\right\} \\ &= \left\{\frac{1}{N} - \frac{2|\beta_m|^2\,\mathrm{Jnr}\,|\mathbf{s}_t^H\mathbf{s}_m|^2/N^2}{(1+N|\beta_m|^2\,\mathrm{Jnr})} + \frac{|\beta_m|^4\,\mathrm{Jnr}^2\,|\mathbf{s}_t^H\mathbf{s}_m|^2/N}{(1+N|\beta_m|^2\,\mathrm{Jnr})^2}\right\} \\ &\approx \frac{1}{N} - \frac{|\mathbf{s}_t^H\mathbf{s}_m|^2}{N^3} \approx \frac{1}{N} \quad (\text{for } N|\beta_m|^2\,\mathrm{Jnr} \gg 1). \end{aligned} \tag{A.6}$$

For $1 + N|\beta_m|^2\,\mathrm{Jnr} \approx 1$, we have

$$\begin{aligned} &\mathbf{w}_1^H\mathbf{w}_1 \\ &\approx \left\{\frac{1}{N} - \frac{2|\beta_m|^2\,\mathrm{Jnr}\,|\mathbf{s}_t^H\mathbf{s}_m|^2}{N^2} + \frac{|\beta_m|^4\,\mathrm{Jnr}^2\,|\mathbf{s}_t^H\mathbf{s}_m|^2}{N}\right\} \\ &= \left\{\frac{1}{N} - \frac{2N|\beta_m|^2\,\mathrm{Jnr}\,|\mathbf{s}_t^H\mathbf{s}_m|^2}{N^3} + \frac{(N|\beta_m|^2\,\mathrm{Jnr})^2|\mathbf{s}_t^H\mathbf{s}_m|^2}{N^3}\right\} \\ &\approx \frac{1}{N}. \end{aligned} \tag{A.7}$$

From (18), we have

$$\mathbf{w}_2^H\mathbf{w}_2 = |\beta_m|^2\sigma_J^4\left[-\mathbf{R}_1^{-1}\mathbf{s}_m + \left(\frac{\mathbf{s}_t^H\mathbf{R}_1^{-1}\mathbf{s}_m}{\mathbf{s}_t^H\mathbf{R}_1^{-1}\mathbf{s}_t}\right)\mathbf{R}_1^{-1}\mathbf{s}_t\right]^H\left[-\mathbf{R}_1^{-1}\mathbf{s}_m + \left(\frac{\mathbf{s}_t^H\mathbf{R}_1^{-1}\mathbf{s}_m}{\mathbf{s}_t^H\mathbf{R}_1^{-1}\mathbf{s}_t}\right)\mathbf{R}_1^{-1}\mathbf{s}_t\right]. \tag{A.8}$$

The dominant term in the expression for $\mathbf{w}_2^H\mathbf{w}_2$ is given by the first term inside the bracket involving $\mathbf{R}_1^{-1}\mathbf{s}_m$, which can be simplified using (24) as

$$\begin{aligned} \mathbf{w}_2^H\mathbf{w}_2 &\approx |\beta_m|^2\sigma_J^4(\mathbf{R}_1^{-1}\mathbf{s}_m)^H(\mathbf{R}_1^{-1}\mathbf{s}_m) \\ &= \frac{|\beta_m|^2\sigma_J^4 N}{(\sigma_n^2+N|\beta_m|^2\sigma_J^2)^2} \\ &= \frac{|\beta_m|^2 N\,\mathrm{Jnr}^2}{(1+N|\beta_m|^2\,\mathrm{Jnr})^2} \\ &\approx \frac{1}{N|\beta_m|^2} \end{aligned} \tag{A.9}$$

for $N|\beta_m|^2\,\mathrm{Jnr} \gg 1$.

The final expression is

$$\mathbf{w}_2^H\mathbf{w}_2 \approx \begin{cases} \dfrac{1}{N|\beta_m|^2} & \text{for } N|\beta_m|^2\,\mathrm{Jnr} \gg 1, \\ N|\beta_m|^2\,\mathrm{Jnr}^2 & \text{for } N|\beta_m|^2\,\mathrm{Jnr} \ll 1. \end{cases} \tag{A.10}$$

We can show that the contributions arising from the three other terms in (A.8) are negligible as follows. The second term in the brackets of (A.8) contains the term $(\mathbf{s}_t^H\mathbf{R}_1^{-1}\mathbf{s}_m/\mathbf{s}_t^H\mathbf{R}_1^{-1}\mathbf{s}_t)\mathbf{R}_1^{-1}\mathbf{s}_t$, the square of which after substituting (26) and (27) takes the following form:

$$\begin{aligned} &|\beta_m|^2\sigma_J^4\left|\frac{\mathbf{s}_t^H\mathbf{R}_1^{-1}\mathbf{s}_m}{\mathbf{s}_t^H\mathbf{R}_1^{-1}\mathbf{s}_t}\right|^2||\mathbf{R}_1^{-1}\mathbf{s}_t||^2 \\ &\quad = \frac{|\beta_m|^2\sigma_n^4\sigma_J^4|\mathbf{s}_t^H\mathbf{s}_m|^2/N^2}{(\sigma_n^2+N|\beta_m|^2\sigma_J^2)^2}||\mathbf{R}_1^{-1}\mathbf{s}_t||^2, \end{aligned} \tag{A.11}$$

where, from (23),

$$\begin{aligned} &||\mathbf{R}_1^{-1}\mathbf{s}_t||^2 \\ &= \frac{1}{\sigma_n^4}\left(\mathbf{s}_t - \frac{\sigma_J^2|\beta_m|^2\mathbf{s}_m\mathbf{s}_m^H\mathbf{s}_t}{\sigma_n^2+N|\beta_m|^2\sigma_J^2}\right)^H\left(\mathbf{s}_t - \frac{\sigma_J^2|\beta_m|^2\mathbf{s}_m\mathbf{s}_m^H\mathbf{s}_t}{\sigma_n^2+N|\beta_m|^2\sigma_J^2}\right) \\ &= \frac{1}{\sigma_n^4}\left(N - \frac{2|\beta_m|^2\,\mathrm{Jnr}\,|\mathbf{s}_m^H\mathbf{s}_t|^2}{1+N|\beta_m|^2\,\mathrm{Jnr}} + \frac{|\beta_m|^4 N\,\mathrm{Jnr}^2\,|\mathbf{s}_m^H\mathbf{s}_t|^2}{(1+N|\beta_m|^2\,\mathrm{Jnr})^2}\right). \end{aligned} \tag{A.12}$$

Simplifying the above expression and finally substituting $1 + N|\beta_m|^2\,\mathrm{Jnr} \approx N|\beta_m|^2\,\mathrm{Jnr}$ we have $\|\mathbf{R}_1^{-1}\mathbf{s}_t\|^2 \approx (N/\sigma_n^4)(1 - |\mathbf{s}_t^H\mathbf{s}_m|^2/N^2) \approx N/\sigma_n^4$. On the other hand, for $N|\beta_m|^2\,\mathrm{Jnr} \ll 1$, we have

$$\begin{aligned}
&\left\|\mathbf{R}_1^{-1}\mathbf{s}_t\right\|^2 \\
&\quad\approx \frac{N}{\sigma_n^4}\left(1 - 2\left|\beta_m\right|^2\left|\mathbf{s}_t^H\mathbf{s}_m\right|^2\frac{\mathrm{Jnr}}{N} + \left|\beta_m\right|^4\left|\mathbf{s}_t^H\mathbf{s}_m\right|^2\mathrm{Jnr}^2\right) \\
&\quad\approx \frac{N}{\sigma_n^4}\left(1 - 2\left(N\left|\beta_m\right|^2\mathrm{Jnr}\right)\frac{\left|\mathbf{s}_t^H\mathbf{s}_m\right|^2}{N^2}\right. \\
&\qquad\left. + \left(N\left|\beta_m\right|^2\mathrm{Jnr}\right)^2\frac{\left|\mathbf{s}_t^H\mathbf{s}_m\right|^2}{N^2}\right) \\
&\quad\approx \frac{N}{\sigma_n^4}.
\end{aligned} \tag{A.13}$$

Back substitution of these expressions in (A.11) and the use of $1 + N|\beta_m|^2\,\mathrm{Jnr} \approx N|\beta_m|^2\,\mathrm{Jnr}$ leads to the expression

$$\begin{aligned}
&\left|\beta_m\right|^2\sigma_f^4\left|\mathbf{s}_t^H\mathbf{R}_1^{-1}\mathbf{s}_m/\mathbf{s}_t^H\mathbf{R}_1^{-1}\mathbf{s}_t\right|^2\left\|\mathbf{R}_1^{-1}\mathbf{s}_t\right\|^2 \\
&\qquad= \frac{\left|\beta_m\right|^2\mathrm{Jnr}^2\left|\mathbf{s}_t^H\mathbf{s}_m\right|^2}{N\left(1 + N\left|\beta_m\right|^2\mathrm{Jnr}\right)^2} \\
&\qquad\approx \frac{\left|\mathbf{s}_t^H\mathbf{s}_m\right|^2/N^2}{N\left|\beta_m\right|^2} \approx 0 \quad \text{for } N\left|\beta_m\right|^2\mathrm{Jnr} \gg 1,
\end{aligned} \tag{A.14}$$

and for $N|\beta_m|^2\,\mathrm{Jnr} \ll 1$, we have

$$\begin{aligned}
&\frac{\left|\beta_m\right|^2\mathrm{Jnr}^2\left|\mathbf{s}_t^H\mathbf{s}_m\right|^2}{N\left(1 + N\left|\beta_m\right|^2\mathrm{Jnr}\right)^2} \\
&\qquad\approx \frac{\left|\beta_m\right|^2\mathrm{Jnr}^2\left|\mathbf{s}_t^H\mathbf{s}_m\right|^2}{N} \approx \left(N\left|\beta_m\right|^2\mathrm{Jnr}^2\right)\frac{\left|\mathbf{s}_t^H\mathbf{s}_m\right|^2}{N^2} \approx 0.
\end{aligned} \tag{A.15}$$

The third contribution in (A.8) is given by (sum of two terms):

$$\begin{aligned}
&-2\,\mathrm{Re}\left\{\frac{\sigma_f^4\left|\beta_m\right|^2\left(\mathbf{s}_m^H\mathbf{R}_1^{-1}\mathbf{s}_t\right)\left(\mathbf{s}_t^H\mathbf{R}_1^{-1}\mathbf{R}_1^{-1}\mathbf{s}_m\right)}{\left(\mathbf{s}_t^H\mathbf{R}_1^{-1}\mathbf{s}_t\right)}\right\} \\
&\qquad= \frac{2\left|\beta_m\right|^2\mathrm{Jnr}^2\left|\mathbf{s}_m^H\mathbf{s}_t\right|^2}{N\left(1 + N\left|\beta_m\right|^2\mathrm{Jnr}\right)^3}.
\end{aligned} \tag{A.16}$$

(Note that replacing $(\mathbf{s}_t^H\mathbf{R}_1^{-1}\mathbf{s}_t)$ by the approximation N/σ_n^2 and with the use of (23), (24), and (26) in (A.16), we arrive at the expression on the right-hand side of (A.16).)

In fact after applying the approximation $1 + N|\beta_m|^2\,\mathrm{Jnr} \approx N|\beta_m|^2\,\mathrm{Jnr}$ or $1 + N|\beta_m|^2\,\mathrm{Jnr} \approx 1$, we can conclude that the right-hand side of (A.16) is approximately equal to zero. From (A.6) and (A.10), the final expression for $\sigma_n^2\|\mathbf{w}\|^2$ is given by (combining (A.6) and (A.10))

$$\sigma_n^2\|\mathbf{w}\|^2 = \begin{cases} \sigma_n^2\left(\dfrac{1}{N} + \dfrac{1}{N\left|\beta_m\right|^2}\right) & \text{for } N\left|\beta_m\right|^2\mathrm{Jnr} \gg 1, \\ \sigma_n^2\left(\dfrac{1}{N} + N\left|\beta_m\right|^2\mathrm{Jnr}^2\right) & \text{for } N\left|\beta_m\right|^2\mathrm{Jnr} \ll 1. \end{cases} \tag{A.17}$$

ACKNOWLEDGMENTS

Authors wish to thank Dr. Dean Prescott and Dr. P. E. Berry for valuable comments and suggestions and Defence Science and Technology Organisation, Australia, for sponsoring this work. We would also like to thank the reviewers for their comments, one of which resulted in the extension in Section 6.1.

REFERENCES

[1] J. Ward, "Space-time adaptive processing for airborn radar," Tech. Rep. TR1015, MIT Lincoln Laboratory, Lexington, Mass, USA, 1994.

[2] S. M. Kogon, E. J. Holder, and D. B. Williams, "Mainbeam jammer suppression using multipath returns," in *Proceedings of 31st Asilomar Conference on Signals, Systems & Computers*, vol. 1, pp. 279–283, Pacific Grove, Calif, USA, November 1997.

[3] Y. Seliktar, E. J. Holder, and D. B. Williams, "An adaptive monopulse processor for angle estimation in a mainbeam jamming and coherent interference scenario," in *Proceedings of IEEE International Conference on Acoustics, Speech, and Signal Processing (ICASSP '98)*, vol. 4, pp. 2037–2040, Seattle, Wash, USA, May 1998.

[4] S. M. Kogon, D. B. Williams, and E. J. Holder, "Exploiting coherent multipath for mainbeam jammer suppression," *IEE Proceedings - Radar, Sonar and Navigation*, vol. 145, no. 5, pp. 303–308, 1998.

[5] R. L. Fante and J. A. Torres, "Cancellation of diffuse jammer multipath by an airborne adaptive radar," *IEEE Transactions on Aerospace and Electronic Systems*, vol. 31, no. 2, pp. 805–820, 1995.

[6] R. A. Gabel, S. M. Kogon, and D. J. Rabideau, "Algorithms for mitigating terrain-scattered interference," *Electronics & Communication Engineering Journal*, vol. 11, no. 1, pp. 49–56, 1999.

[7] R. Schmidt, "Multiple emitter location and signal parameter estimation," *IEEE Transactions on Antennas and Propagation*, vol. 34, no. 3, pp. 276–280, 1986.

[8] H. L. Van Trees, *Optimum Array Processing, Part IV of Detection, Estimation, and Modulation Theory*, John Wiley & Sons, New York, NY, USA, 2002.

[9] D. Madurasinghe, "Performance analysis of an airborne high PRF phased array radar in a jamming environment," in *Proceedings of International Conference on Radar*, pp. 323–326, Adelaide, SA, Australia, September 2003.

Dan Madurasinghe received the B.S. (physics) and B.S. (maths. hon) (first class) degrees from the University of Sri Lanka in 1978 and 1980, respectively; the M.S. degree in computer science from the Asian Institute of Technology, Bangkok, Thailand, in 1982; the Ph.D. degree in applied mathematics and the Grad.Dip. degree in telecommunications from the University of Adelaide, Australia, in 1987 and 1991, respectively. From 1987 to 1988, he held the Australian National Research Fellowship (postdoctoral) to conduct research in mathematical modeling of corrosion degradation processes. In 1988, he joined the Defence Science and Technology Organisation (DSTO), Australia, as a Research Scientist where he worked on the application of antenna array processing techniques in radio direction finding. In 1991, he was promoted to the position of Senior

Research Scientist at the Electronics Warfare and Radar Division, DSTO. His current research involves multichannel radar signal-processing algorithms for airborne radar.

Andrew P. Shaw received a first-class honours degree in physics from the University of Reading, UK, in 1983, and a Ph.D. degree in 1987. From 1986 until 2002, he worked in the UK MOD research establishments, where he worked on a diverse range of sensor programmes. Since 2002, he has been the Research Leader in microwave radar at the Defence Science and Technology Organisation, Australia. Shaw is a Member of the Institute of Physics, a Chartered Scientist, and a Chartered Physicist.